2018 Annual American Control Conference (ACC)
June 27–29, 2018. Wisconsin Center, Milwaukee, USA

Output-Feedback Adaptive Control of Discrete-Time Systems with Unmodeled, Unmatched, Inaccessible Nonlinearities

Syed Aseem Ul Islam and Dennis S. Bernstein

Abstract— **We present a numerical investigation of output-feedback discrete-time adaptive control for a class of nonlinear systems. Systems with unknown nonlinearities that may be unmatched with the control are considered. The unknown nonlinearity is assumed to be inaccessible in the sense that it is a function of states that are not measured. For these systems, retrospective cost adaptive control is used for output-feedback stabilization, command following, and disturbance rejection.**

I. Introduction

Although feedback control of nonlinear systems has seen major advances over the past decades, most methods assume either full-state feedback or fully known dynamics. The present paper approaches output-feedback control of nonlinear systems from the perspective of adaptive control, which focuses on the case where the dynamics are poorly modeled, including the possibility of unmodeled nonlinearities. This setting precludes the use of model-dependent techniques.

In the present paper we consider output-feedback control of discrete-time nonlinear systems using retrospective cost adaptive control (RCAC), which was developed for linear systems in [1]–[3]. In [4], RCAC was applied to harmonic command following for the van der Pol and Duffing oscillators. This investigation was naive in the sense that no effort was made to account for the presence of the nonlinearity.

Close examination of the control signals for the van der Pol and Duffing oscillators in [4] reveals that the RCAC controller, which, after convergence, is linear time-invariant (LTI), approximately cancels the effect of the unmodeled nonlinearity. For these systems, cancellation is achievable in principle due to the fact that the nonlinearities are matched. Nevertheless, for harmonic command following, an attempt to cancel an unknown nonlinearity may lead to the generation of higher, spurious harmonics, which also must be rejected. RCAC must therefore adapt the control so as to follow the harmonic command while suppressing the spurious harmonics generated by the unmodeled nonlinearity.

As a further step toward understanding how RCAC accounts for unmodeled nonlinearities, this paper presents a numerical investigation of RCAC for a class of nonlinear control problems. In particular, we consider step and harmonic command following, and step, harmonic, and stochastic disturbance rejection with various nonlinearities, including nonlinear functions that are either smooth, continuous but not differentiable, or discontinuous. In addition, the examples in the present paper are characterized by three notable features. First, the nonlinearity is assumed to be unknown and unmodeled. This assumption precludes the use of nonlinear control methods that use knowledge of the nonlinearity. Next, we consider the case where the control and nonlinearity drive the system differently; in other words, the control and nonlinearity are unmatched. This assumption precludes the possibility that the RCAC controller can directly cancel the effect of the nonlinearity. Finally, we consider the case where the nonlinearity is a function of states that are not measured. In this case, the nonlinearity is *inaccessible*. This assumption implies that, even if the nonlinearity were known and matched, it would be impossible for the control to cancel it without the use of state estimates. In fact, for all of the examples in this paper, the full state is not measured, and thus the RCAC controller is an output-feedback control law.

Syed Aseem Ul Islam and Dennis S. Bernstein are with the Department of Aerospace Engineering, University of Michigan, Ann Arbor, MI, USA. {aseemisl, dsbaero}@umich.edu

II. The Adaptive Servo Problem for a Class of Nonlinear Plants

We consider the discrete-time, nonlinear plant

$$x(k+1) = Ax(k) + Bu(k) + B_{\rm nl}f(x(k)) + D_{\rm d}d(k), \quad (1)$$

$$y_0(k) = Cx(k), \quad (2)$$

$$y_{\rm n}(k) = y_0(k) + v(k), \quad e_0(k) = r(k) - y_0(k), \quad (3)$$

$$z(k) \triangleq r(k) - y_{\rm n}(k) = e_0(k) - v(k), \quad (4)$$

where $x(k) \in \mathbb{R}^n$ is the state, $u(k) \in \mathbb{R}^{l_u}$ is the control input, $f\colon \mathbb{R}^n \to \mathbb{R}$ is a nonlinear function, $d(k) \in \mathbb{R}^{l_d}$ is the disturbance, $y_0(k) \in \mathbb{R}^{l_y}$ is plant output, $y_{\rm n}(k) \in \mathbb{R}^{l_y}$ is the measurement, $e_0(k) \in \mathbb{R}^{l_y}$ is the true error, $r(k) \in \mathbb{R}^{l_y}$ is the command, $v(k) \in \mathbb{R}^{l_y}$ is the sensor noise, and $z(k) \in \mathbb{R}^{l_y}$ is the measured error, which is also the performance variable.

The nonlinear plant (1), (2) can be written as

$$y_0(k) = \mathcal{G}(\mathbf{q}) \begin{bmatrix} u^{\rm T}(k) & d^{\rm T}(k) & f^{\rm T}(x(k)) \end{bmatrix}^{\rm T}, \quad (5)$$

where $\mathbf{q}$ is the forward shift operator, $\mathcal{G} \triangleq \begin{bmatrix} G & G_{\rm nl} \end{bmatrix}$, $G \triangleq \begin{bmatrix} G_{y_0u} & G_{y_0d} \end{bmatrix}$, $G_{\rm nl}(\mathbf{q}) \triangleq C(\mathbf{q}I - A)^{-1}B_{\rm nl}$, $G_{y_0u}(\mathbf{q}) \triangleq C(\mathbf{q}I-A)^{-1}B$, and $G_{y_0d}(\mathbf{q}) \triangleq C(\mathbf{q}I-A)^{-1}D_{\rm d}$. If f is absent, the $\mathcal{G} = G$. The control input is given by

$$u(k) = G_{{\rm c},k}(\mathbf{q})z(k), \quad (6)$$

where the discrete-time, linear-time-varying (LTV) transfer function $G_{{\rm c},k}$ is the adaptive controller at step k. For pole-zero analysis, $\mathbf{q}$ can be replaced by the Z-transform variable $\mathbf{z}$. Figure 1 represents the nonlinear function f as a feedback loop around the linear system $\mathcal{G}$. For convenience, we refer to $\mathcal{G}$ as the nonlinear plant, that is, (1), (2) with f present.

978-1-5386-5427-9/$31.00 ©2018 AACC

The error signal z is the difference between the command r and the measurement $y_{\rm n}$, which may be corrupted by noise. Since this is the only error signal available for feedback, it serves as the performance variable for the adaptive controller. However, the error signal e_0, which is the difference between the command r and the plant output y_0, provides a true measure of the command-following performance. Since this signal is not available for feedback, it is used only as a diagnostic. If sensor noise is absent, then $z \equiv e_0$.

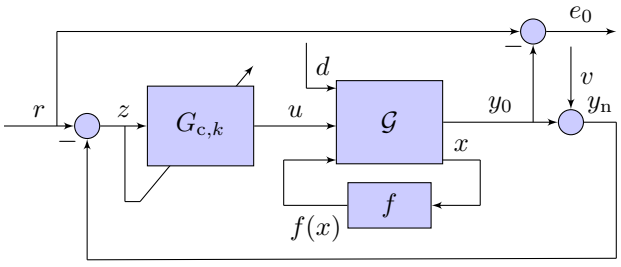

Fig. 1: Block diagram representation of the adaptive servo problem with the adaptive controller $G_{c,k}$ and the nonlinear plant $\mathcal{G}$ given by (1), (2).

III. Adaptive Control Algorithm

RCAC requires limited modeling data for SISO linear plants, namely, the sign of the leading numerator coefficient, the relative degree, and the locations of nonminimum-phase (NMP) zeros, if any. This modeling information is used to construct the filter $G_{\rm f}$, which serves as a target model for the intercalated transfer function, as explained in [4]. The controller order $n_{\rm c}$ as well the adaptation weight R_θ and control weight R_u must also be specified. As in [4], the controller coefficient matrix θ is initialized to be zero at the start of all numerical examples; this assumption reflects the absence of additional modeling information. Details of RCAC and its implementation using recursive least squares to update θ are given in [4].

IV. Numerical Examples

We consider $3^{\rm rd}$-order asymptotically stable linear dynamics, where (A, B, C) is minimal and G_{y_0u} is minimum phase with relative degree 1. The vector $B_{\rm nl}$ is chosen for each example in order to consider nonlinearities f that are either matched or unmatched with the control input, that is, $B_{\rm nl} = B$ or $B_{\rm nl} \neq B$, respectively. Note that, in the case where f is unmatched, it is impossible for u to directly cancel the effect of f. The nonlinearity f is represented as $f(x) = \alpha f_0(x)$, where $\alpha \in \mathbb{R}$ is varied to assess the impact of f on stability and performance.

We are primarily interested in the case where f depends on components of x that are not measured; in this case, f is *inaccessible*. Consequently, if f is matched but inaccessible, then u cannot use the measurements $y_{\rm n}$ to cancel f without estimating unmeasured states. For all of the examples in this paper, f is inaccessible. This assumption precludes the use of feedback linearization whether or not f is known.

For each example, f is unmodeled, and the goal is to determine the ability of RCAC to account for the presence of f. We consider command following with step and harmonic commands as well as disturbance rejection with step, harmonic, and stochastic disturbances.

Since f is unmodeled, we choose $G_{\rm f}$ based on the modeling information needed by RCAC in the case $f = 0$. We thus set [4]

$$G_{\rm f}(\mathbf{q}) = -\mathbf{q}^{-1}, \tag{7}$$

where $G_{\rm f}$ captures the relative degree, NMP zeros (none in the minimum phase case), and sign of the leading numerator coefficient of G_{y_0u}. The minus sign in (7) arises due to (4).

V. Comparison of RCAC and LQG for Cubic f

In this section we apply RCAC to $\mathcal{G}$ in the case where f is a matched cubic nonlinearity. The goal is to determine how the final RCAC controller accounts for the effect of f. To do this, we first design an LQG controller based only on the linear plant G, where the LQG controller is constructed to include an internal model of the command. Since the LQG controller is designed without regard to f, there is no stability or performance guarantee when it is applied to $\mathcal{G}$. Nevertheless, applying the LQG controller to $\mathcal{G}$ for various values of α provides a measure of the inherent robustness of LQG to f. This provides a baseline comparison of the performance of RCAC relative to LQG with f present.

Next, RCAC is applied to the nonlinear plant $\mathcal{G}$, and the final RCAC controller is saved as an LTI controller. We then apply the final RCAC controller (and thus without further adaptation) to the nonlinear plant $\mathcal{G}$ and compare its performance to the performance of the LQG controller as applied to the same nonlinear plant $\mathcal{G}$. In particular, we analyze the spectral content of e_0 and u in order to determine how the final RCAC controller accounts for the effect of f.

We consider command following with the harmonic command $r(k) = \cos \omega_r k$, where $\omega_r = 0.2$ rad/sample. No disturbance is present. The nonlinearity f is given by $f(x) = \alpha x_1^3$, where α is chosen below. We set

$$x \triangleq \begin{bmatrix} x_1 \\ x_2 \\ x_3 \end{bmatrix}, \quad A = \begin{bmatrix} 0 & 0 & 0.784 \\ 1 & 0 & -2.287 \\ 0 & 1 & 2.434 \end{bmatrix}, \tag{8}$$

$$B = \begin{bmatrix} 0.12 \\ -0.7 \\ 1 \end{bmatrix}, \quad C = \begin{bmatrix} 0 & 0 & 1 \end{bmatrix}. \tag{9}$$

Note that G_{y_0u} has the real pole 0.801 rad/sample and the lightly damped poles $0.817 \pm 0.559\jmath$ rad/sample, which have a frequency of 0.6 rad/sample. The zeros of (8), (9) are 0.3 rad/sample and 0.4 rad/sample. Finally, $B_{\rm nl} = B$, and thus f is matched. For simplicity, we assume $x(0) = 0$. Assuming that x_1 is harmonic with frequency ω_r, note that

$$f(\sin \omega_r k) = \alpha \sin^3 \omega_r k = \frac{3\alpha}{4} \sin \omega_r k + \frac{\alpha}{4} \sin 3\omega_r k.$$

Therefore, f generates a harmonic signal at the frequency $3\omega_r$. Since these signals occur in the closed-loop system, the signal $f(\frac{3}{4} \sin \omega_r k + \frac{1}{4} \sin 3\omega_r k)$ produces additional spectral content at the frequencies $5\omega_r$ and $7\omega_r$, which, in turn, produces further spectral content. These signals appear as unmodeled disturbances, which may need to be suppressed by the controller. Note that the plant (8), (9) is chosen to have a pair of lightly damped poles at the frequency $3\omega_r = 0.6$

rad/sample. Consequently, (8), (9) is highly sensitive to the effect of f for the given command frequency.

To construct the LQG controller we augment the linear plant G_{y_0u} with an internal model of the harmonic command, which yields an augmented plant of order 5. We design an LQG controller for this 5th-order plant using the MATLAB function `lqg(sys,`Q_{xu}, Q_{wv}`)` with $Q_{xu} = \mathrm{diag}[0\ 0\ 1000\ 0\ 0\ 1], Q_{wv} = I_6$, where `sys` is a MATLAB representation of the augmented plant with the first two states representing the internal model. The resulting LQG controller is then cascaded with the internal model to yield a final controller of order 7. This controller is then applied to the nonlinear plant $\mathcal{G}$. Note that the LQG controller with the internal model requires knowledge of the frequency of the command; this information is not needed for the RCAC controller. Furthermore, as discussed above, RCAC requires limited information about (A, B, C), whereas the LQG controller requires complete knowledge of these matrices.

For RCAC we set $n_c = 14$, $R_\theta = 0.0002$, and $R_u = 0.01$. The error e_0 approaches zero (not shown) for the parameters $\alpha \in [-0.034, 0.062]$ and $\alpha \in [-0.550, 0.309]$, for the LQG controller and RCAC, respectively. In particular, Figure 2 shows the error e_0 for both controllers with $\alpha = 0.05$.

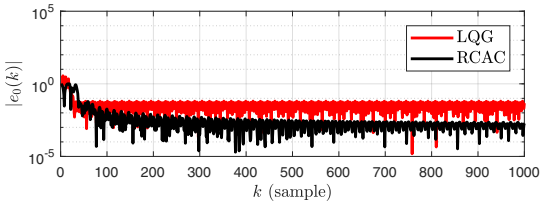

Fig. 2: For $\alpha = 0.05$, $|e_0(k)|$ is plotted for both LQG and RCAC.

Next, for $\alpha = 0.062$, which represents the largest value of α for which e_0 is bounded using the LQG controller, we simulate the closed-loop system using both controllers. We record the final RCAC controller $G_{c,10,000}$ and rerun the simulation with this LTI controller.

To compare the LQG controller to the LTI RCAC controller $G_{c,10,000}$, we compute the power spectral density (PSD) of e_0 and u using the MATLAB function `periodogram` for the last 9,000 steps of the simulations, as shown in Figure 3. The frequency response of G_{y_0u}, the LQG controller, and $G_{c,10,000}$ are shown in Figure 4(a), and the frequency response of the sensitivity functions corresponding to both controllers are shown in Figure 4(b).

Figure 3(a) shows that, relative to the LQG controller, the LTI RCAC controller $G_{c,10,000}$ reduces the error z at all frequencies except at the command frequency 0.2 rad/sample, where its performance is slightly worse. In particular, $G_{c,10,000}$ suppresses e_0 at 0.6 rad/sample significantly more than the LQG controller. Of course, the LQG controller is not aware of the presence of the "disturbance" at $3\omega_r$. It is possible to redesign the LQG controller to include an internal model at both ω_r and $3\omega_r$, resulting in a controller of order 11. However, this would require knowledge of both ω_r and f. It can be seen in Figure 4(a) that $G_{c,10,000}$ has higher magnitude at 0.6 rad/sample than the LQG controller.

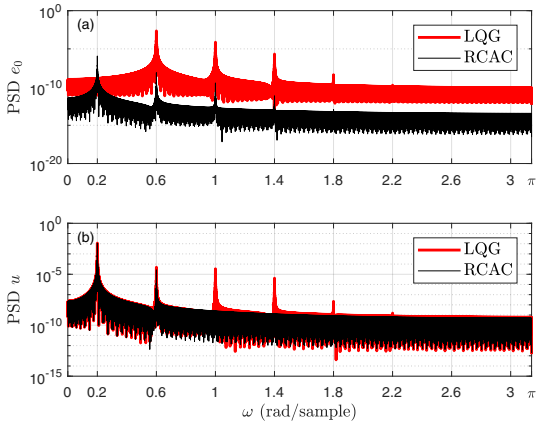

Fig. 3: For each controller, (a) shows the PSD estimate (in sample/rad) for e_0; (b) shows the PSD estimate (in sample/rad) for u.

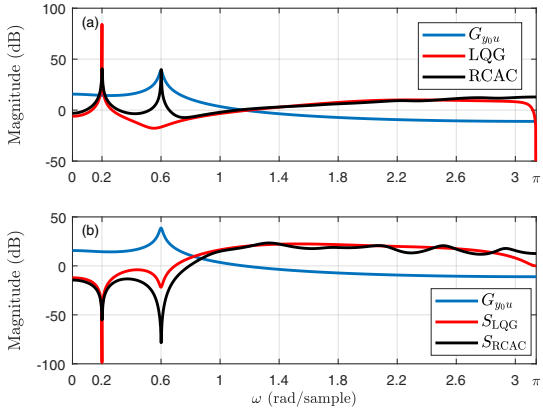

Fig. 4: (a) shows the frequency response of G_{y_0u}, the LQG controller, and the final RCAC controller $G_{c,10,000}$. (b) shows the frequency response of G_{y_0u} and the sensitivity functions corresponding to both controllers.

Consequently, in Figure 4(b) there is a deeper notch at 0.6 rad/sample in the sensitivity S_{RCAC} corresponding to $G_{c,10,000}$ compared to the sensitivity S_{LQG} corresponding to the LQG controller. As a consequence of the discrete-time Bode sensitivity integral, the notch in S_{RCAC} is less deep than the notch in S_{LQG} at 0.2 rad/sample. This is the reason that $G_{c,10,000}$ has slightly worse performance than the LQG controller at 0.2 rad/sample, but significantly better performance at all other frequencies.

VI. Command Following Examples

For all examples in Sections VI and VII, we use the same RCAC tuning parameters; no attempt is made to refine the RCAC weightings for each example. In particular, we set $n_c = 3$, $R_\theta = 0.002$, and $R_u = 0.01$, and use the target model (7). In addition, we set

$$x \triangleq \begin{bmatrix} x_1 \\ x_2 \\ x_3 \end{bmatrix}, \quad A = \begin{bmatrix} 0 & 0 & 0.40 \\ 1 & 0 & -1.62 \\ 0 & 1 & 2.20 \end{bmatrix}, \tag{10}$$

$$B = \begin{bmatrix} 0.12 \\ -0.7 \\ 1 \end{bmatrix}, \quad C = \begin{bmatrix} 0 & 0 & 1 \end{bmatrix}. \tag{11}$$

Note that G_{y_0u} has poles $\{0.8, 0.7 \pm 0.1\jmath\}$ rad/sample, and zeros $\{0.3, 0.4\}$ rad/sample.

The examples in this section are for step and harmonic

command following with $d(k) = 0$. For each example, the command is either a step $r(k) = \beta$ or a harmonic $r(k) = \beta \cos \omega_r k$, where $\omega_r > 0$, and the initial condition is $x(0) = \gamma[1 \quad 1 \quad 1]^{\mathrm{T}}$. The nominal parameters are $\alpha = 0.1$, $\beta = 1$, $\gamma = 0$, and $\omega_r = 0.2$ rad/sample. In examples 2 and 4 we test robustness by individually varying α, β, and γ with the remaining parameters fixed at their nominal values. The goal is to determine the range of values of α, β, and γ for which the command is followed asymptotically. Sensor noise is assumed to be absent for the examples in this section, but is included in Section VII. Table I summarizes the examples in this section. Except for Example 1, all examples in the paper involve unmatched nonlinearities.

TABLE I: Summary of command-following examples.

Example	f_0	f Matched?	Command
1	$x_1^2 + 1$	Yes	harmonic
2	$\lvert x_1 x_2 \rvert$	No	step
3	$\operatorname{sgn}(x_2)$	No	harmonic
4	e^{x_1}	No	harmonic
5	$\begin{bmatrix} \frac{1}{\lvert x_1 \rvert + 1} \\ \log(1 + 5x_2^2) \end{bmatrix}$	No	Harmonic

Example 1. *Harmonic command following with a quadratic-plus-bias matched nonlinearity.* Let $f_0(x) = x_1^2 + 1$ and $B_{\mathrm{nl}} = B$. To evaluate the effect of the control input u for the nonlinear plant, we first apply RCAC to the linear plant, that is, with $f = 0$, and obtain the control input u_{lin} produced by the RCAC controller for the linear plant. By comparing u to u_{lin}, we can determine how RCAC, as applied to the nonlinear plant, modifies the control input in order to account for the presence of f. For the nominal parameters $\alpha, \beta, \gamma, \omega_r$, Figure 5 shows that RCAC follows the harmonic command. Figure 6 shows that RCAC generates a control signal u for the nonlinear plant such that $u+f$ is close to u_{lin}. This shows that, in the matched case, the control generated by RCAC for the nonlinear plant works together with the inaccessible nonlinearity to produce a control signal that approximates the control signal for the linear plant. In effect, RCAC cancels f despite the fact that f is unknown and $f(0) \neq 0$. ◇

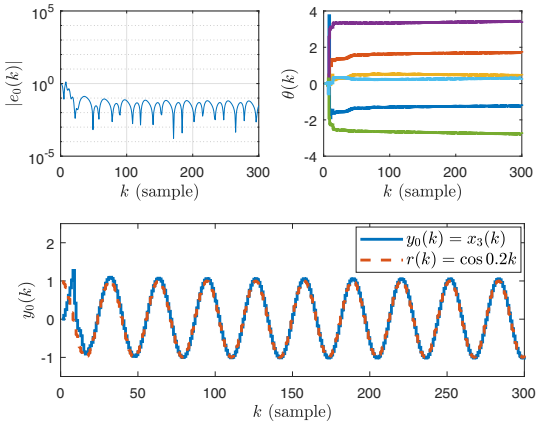

Fig. 5: Example 1: Harmonic command following for $f_0(x) = x_1^2 + 1$ with the nominal parameters. After a transient of about 20 steps, RCAC follows the harmonic command.

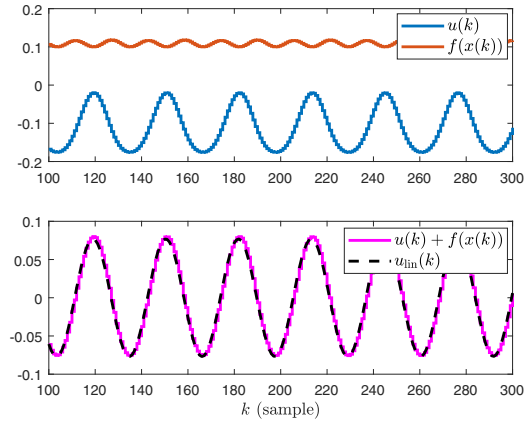

Fig. 6: Example 1: Control input corresponding to Figure 5. The control signal $u(k)$ for the nonlinear system satisfies $u(k) + f(x(k)) \approx u_{\mathrm{lin}}(k)$.

Example 2. *Step command following with a continuous-but-nondifferentiable unmatched nonlinearity.* Let $f_0(x) = |x_1 x_2|$ and $B_{\mathrm{nl}} = [-1 \;\; 0 \;\; 0]^{\mathrm{T}}$. For the nominal values of α, β, γ, ω_r, Figure 7 shows that RCAC follows the step command. Next, we vary α, β, γ one at a time with the remaining parameters set to their nominal values. The resulting behavior of e_0 (not shown) for $\alpha \in [-0.35, 0.58]$, $\beta \in [-3.73, 5.54]$, and $\gamma \in [-0.22, 0.55]$ is similar to Figure 7. This provides an estimate of the region of convergence of RCAC in terms of the parameters α, β, γ.

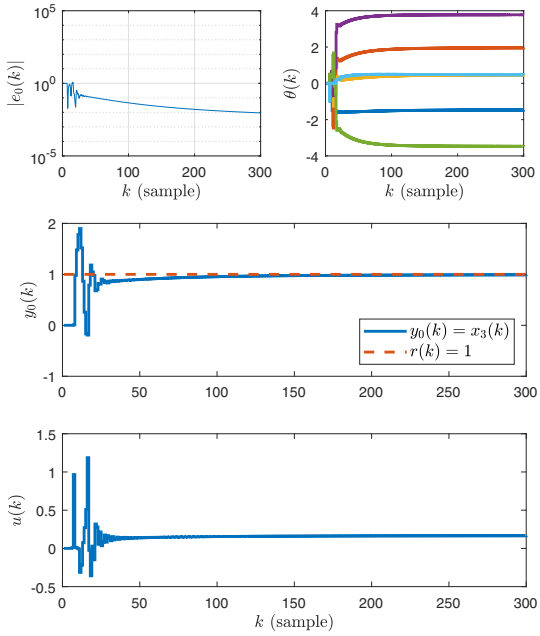

Fig. 7: Example 2: Step command following for $f_0(x) = |x_1 x_2|$ with the nominal parameters. After the transient, RCAC follows the step command.

Next, we examine the performance of the final controller $G_{\mathrm{c},300}$ corresponding to Figure 7 by applying it as an LTI controller to the nonlinear plant. Using $G_{\mathrm{c}} = G_{\mathrm{c},300}$ from $k = 0$, the behavior of e_0 (not shown) is similar to Figure 7 for the values $\alpha \in [-0.31, 0.28]$, $\beta \in [-3.12, 2.92]$, $\gamma \in [-1.70, 2.34]$ varied as described above. This provides an estimate of the region of convergence of the final controller $G_{\mathrm{c}} = G_{\mathrm{c},300}$ in terms of the parameters α, β, γ. ◇

Example 3. *Harmonic command following with a discontinous unmatched nonlinearity.* Let $f_0(x) = \operatorname{sgn}(x_2)$,

$B_{\rm nl} = [-1 \;\; 0 \;\; 0]^{\rm T}$, and

$$\omega_r = \begin{cases} 0.2 \text{ rad/sample}, & k \leq 150, \\ 0.4 \text{ rad/sample}, & k > 150. \end{cases} \tag{12}$$

For the nominal parameters α, β, γ, Figure 8 shows that RCAC follows the harmonic command. In particular, RCAC readapts at $k = 150$ to account for the change in the command frequency. ◇

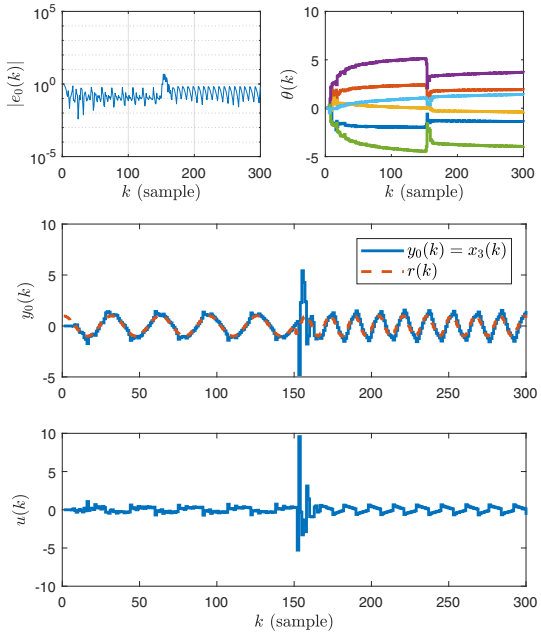

Fig. 8: Example 3: Harmonic command following with the discontinuous nonlinearity $f_0(x) = \text{sgn}(x_2)$ using the nominal parameter values. RCAC adapts to the abrupt change in command frequency at step $k = 150$.

Example 4. *Harmonic command following with a time-varying, exponential, unmatched nonlinearity.* Let $f_0(x) = e^{x_1}$ and $B_{\rm nl} = [-1 \;\; 0 \;\; 0]^{\rm T}$, and vary α as

$$\alpha(k) = \begin{cases} -0.27\frac{k}{300}, & k \leq 300, \\ -0.27, & k > 300, \end{cases} \tag{13}$$

with the remaining parameters set to their nominal values. We thus write $f(k, x) = \alpha(k) f_0(x)$ in place of $f(x)$. Figure 9 shows that RCAC follows the harmonic command in the presence of the time-varying nonlinearity.

Note that the final value -0.27 of α in (13) is less than the most negative fixed value -0.15 of α for which RCAC is able to stabilize the plant. ◇

Example 5. *Harmonic command following with an unmatched vector nonlinearity.* Define

$$B_{\rm nl} = \begin{bmatrix} 1 & 0 \\ 0 & 1 \\ 0 & 0 \end{bmatrix}, \quad f_0(x) = \begin{bmatrix} \frac{1}{|x_1|+1} \\ \log(1 + 5x_2^2) \end{bmatrix}. \tag{14}$$

Note that f_0 has two components, and both components are unknown, unmatched, and inaccessible. For the nominal parameters α, β, γ, ω_r, Figure 10 shows that RCAC follows the harmonic command. ◇

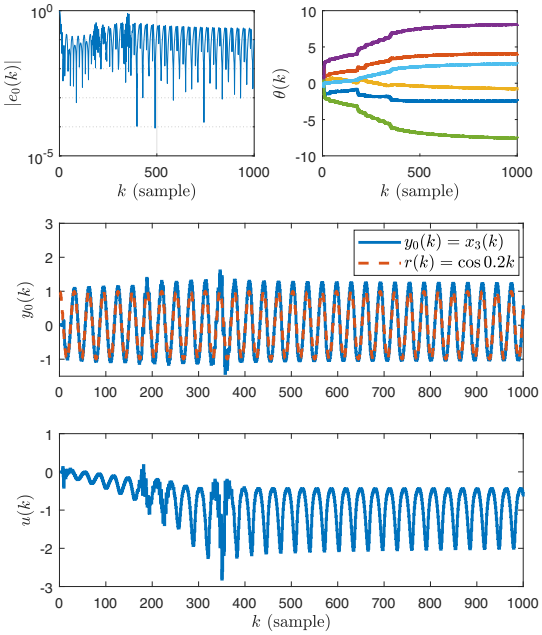

Fig. 9: Example 4: Harmonic command following for $f(k, x) = -\alpha(k)e^{x_1}$, where α varies according to (13). The remaining parameters are set to their nominal values.

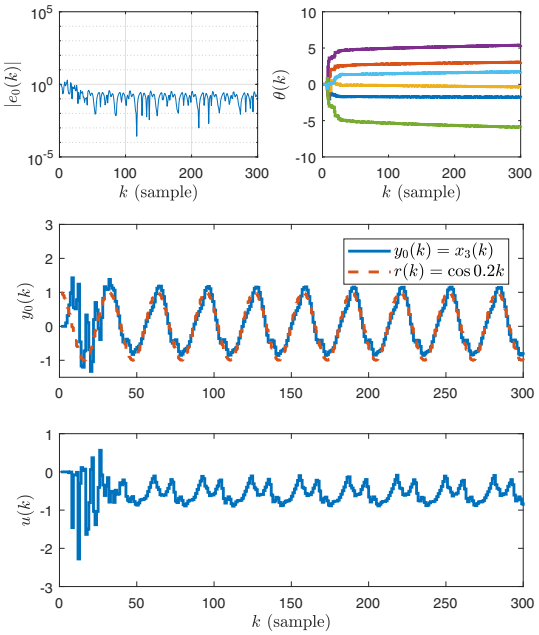

Fig. 10: Example 5: Harmonic command following with the vector nonlinearity (14) both of whose components are unmatched and inaccessible using the nominal parameter values.

VII. Disturbance Rejection Examples

We now consider disturbance rejection with step, harmonic, and stochastic disturbances and with $r(k) = 0$. In contrast to the command-following examples in Section VI, we now set $v \sim N(0, 0.01^2)$ to simulate sensor noise. For all examples in this section, let $B_{\rm nl} = [-1 \;\; 0 \;\; 0]^{\rm T}$ so that f is unmatched. In addition, for each example, the disturbance may or may not be matched with the control, that is, $D_{\rm d} = B$ or $D_{\rm d} \neq B$, respectively. Let $d = \delta d_0$, and, as in the case of command following, $f = \alpha f_0$. For each example, the nominal parameters are $\alpha = 2.00$, $\delta = 0.10$, and, for

examples 6 and 7, we individually vary α and δ with the remaining parameter fixed at its nominal value to determine the range of values for which RCAC rejects the disturbance. For simplicity, we set $x(0) = 0$ for all examples. Therefore, the domain of attraction is not investigated for the examples in this section. Table II summarizes the examples in this section, where $\tau > 0$ is the saturation level.

TABLE II: Summary of disturbance-rejection examples.

Example	f_0	Disturbance
6	$\operatorname{sgn}(x_1)\lvert x_1\rvert^{\frac{1}{2}}$	step
7	$\sin(x_2)$	harmonic
8	$\operatorname{sat}_\tau(x_1)$	broadband

Example 6. *Step disturbance rejection with a nonlipschitzian nonlinearity.* Let $f_0(x) = \operatorname{sgn}(x_1)\lvert x_1\rvert^{\frac{1}{2}}$, for all $k \geq 0$, $d_0(k) = 1$, and $D_\mathrm{d} = B$ so that u and d are matched. For the nominal values of α and δ, Figure 11 shows that RCAC rejects the step disturbance in the presence of sensor noise. Next, we vary α and δ one at a time with the remaining parameter set to its nominal value. The resulting behavior of e_0 (not shown) for $\alpha \in [-1.79, 4.58]$ and $\delta \in [-1.49, 1.23]$ is similar to Figure 11. ◇

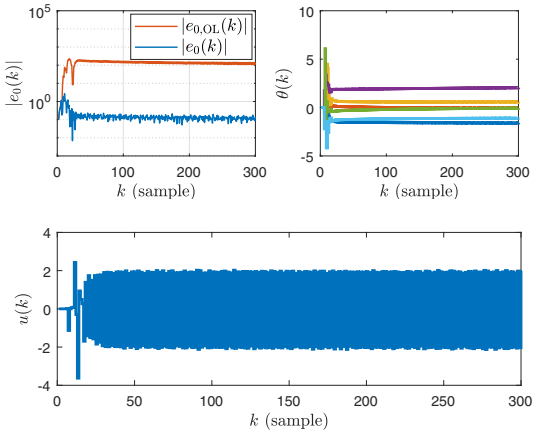

Fig. 11: Example 6: Step disturbance rejection for $f_0(x) = \operatorname{sgn}(x_1)\lvert x_1\rvert^{\frac{1}{2}}$ with the nominal parameter values. The absolute open-loop true error $\lvert e_{0,\mathrm{OL}}(k)\rvert$ and the absolute closed-loop true error $\lvert e_0(k)\rvert$ are shown together for contrast. The signal-to-noise ratio (SNR) for y_0 and v is 17.99.

Example 7. *Harmonic disturbance rejection with a harmonic nonlinearity.* Let $f_0(x) = \sin x_2$, $D_\mathrm{d} = [0 \;\; 0 \;\; 1]^\mathrm{T}$, $v \sim N(0, 0.08^2)$, and $d_0(k) = \sin 0.32k$. For the nominal α and δ, Figure 12 shows that RCAC rejects the harmonic disturbance in the presence of sensor noise. Using RCAC, the error e_0 is similar to Figure 12 (not shown) for all values of α and δ, where each parameter is varied individually with the remaining parameter fixed at its nominal value.

Next, we vary α and δ one at a time with the remaining parameter set to its nominal value. The resulting behavior of e_0 (not shown) for all values of α, δ is similar to Figure 12.

Next, we examine the performance of the final controller $G_{\mathrm{c},600}$ corresponding to Figure 12 by applying it as an LTI controller to the nonlinear plant. Using $G_{\mathrm{c},600}$ from $k = 0$, the behavior of e_0 (not shown) is similar to Figure 12 for all values of α and δ, varied as described above. ◇

Example 8. *Broadband disturbance rejection with a saturation nonlinearity.* Let $f_0(x) = \operatorname{sat}_{0.02}(x_1)$, $D_\mathrm{d} = [0 \;\; 0 \;\; 1]^\mathrm{T}$, and $d_0 \sim N(0, 1^2)$. For the nominal values of α and δ, Figure 13 shows that RCAC rejects the broadband disturbance in the presence of sensor noise. ◇

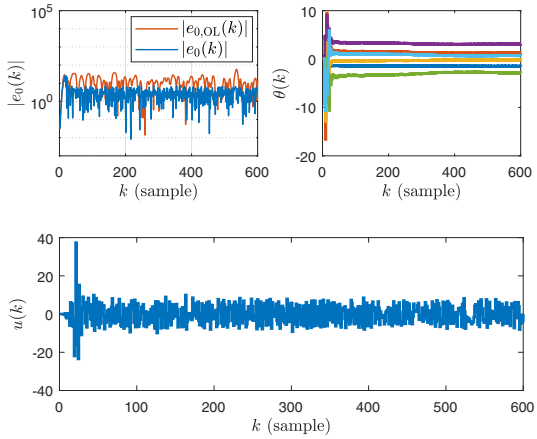

Fig. 12: Example 7: Harmonic disturbance rejection for $f_0(x) = \sin x_2$ with the nominal parameter values. The absolute open-loop true error $\lvert e_{0,\mathrm{OL}}(k)\rvert$ and the absolute closed-loop true error $\lvert e_0(k)\rvert$ are shown together for contrast. The SNR is 53.56.

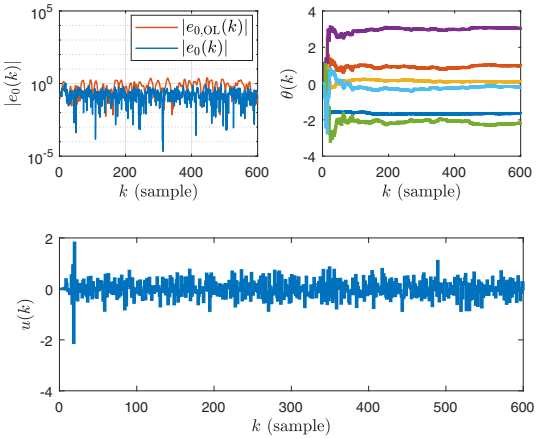

Fig. 13: Example 8: Broadband disturbance rejection for $f_0(x) = \operatorname{sat}_{0.02}(x_1)$ with the nominal values of parameters. The absolute open-loop true error $\lvert e_{0,\mathrm{OL}}(k)\rvert$ and the absolute closed-loop true error $\lvert e_0(k)\rvert$ are shown together for contrast. The SNR is 25.84.

VIII. Conclusions

This paper provided a numerical investigation of output-feedback adaptive control of nonlinear plants with unmatched, inaccessible nonlinearities. Under extremely limited modeling information, which assumed no knowledge of the nonlinearity, RCAC was able to stabilize, follow step and harmonic commands, and reject step, harmonic, and stochastic disturbances for various nonlinearities. Future research will consider plants that are open-loop unstable and nonminimum phase.

References

[1] M. A. Santillo and D. S. Bernstein, "Adaptive Control Based on Retrospective Cost Optimization," *J. Guid. Contr. Dyn.*, vol. 33, pp. 289–304, 2010.

[2] J. B. Hoagg and D. S. Bernstein, "Retrospective Cost Model Reference Adaptive Control for Nonminimum-Phase Systems," *J. Guid. Contr. Dyn.*, vol. 35, pp. 1767–1786, 2012.

[3] R. Venugopal and D. S. Bernstein, "Adaptive Disturbance Rejection Using ARMARKOV System Representations," *IEEE Trans. Contr. Sys. Tech.*, vol. 8, pp. 257–269, 2000.

[4] Y. Rahman, A. Xie, and D. S. Bernstein, "Retrospective Cost Adaptive Control: Pole Placement, Frequency Response, and Connections with LQG Control," *IEEE Contr. Sys. Mag.*, vol. 37, pp. 28–69, Oct. 2017.